ECONTECHMOD. AN INTERNATIONAL QUARTERLY JOURNAL – 2018, Vol. 07, No. 4, 29 – 36

Angle of injection impact on the combustion process in a compression-ignition engine

P. Łagowski[1], D. Kurczyński[1], G. Wcisło[2,3], B. Pracuch[3], V. Tomyuk[4]

[1] *Kielce University of Technology*
Department of Automotive Vehicles and *Transportation, Poland*
Phone: 0048 41 3424332
e-mail: kdarek@tu.kielce.pl
[2]*Faculty of Production Engineering and Power Technologies. University of Agriculture in Krakow, Poland*
Phone. 0048 513-157-977,
e-mail: grzegorz.wcislo@ur.krakow.pl
[3] *Malopolskie Centre for Renewable Energy Sources "BioEnergia", Poland*
e-mail: gwcislo@bioenergia.com.pl
[4] *Lviv National Agrarian University; Department of Automobiles and Tractors*
e-mail: vtomyuk@ukr.net

Received December 01.2018: accepted December 22.2018

*Abstract***.** The article presents the impact of hydrocarbon fuel angle of injection on heat emission characteristics in a compression - ignition AD3.152 engine. The angle of injection has a significant impact on the primary engine operating parameters and combustion process indicators, which include the proportion of combustion which occurs according to kinetic and diffusion models, heat emission rate and the combustion process duration. The characteristics describing emission of a relative heat quantity were determined on the basis of an analysis of actual, indicator diagrams averaged over 100 runs, under the assumption that the combustion process ends by the time the exhaust valve opens. During the test, the engine operated according to an external speed characteristic. Tests were carried out for three fuel angles of injection: 13, 17 and 21 crankshaft rotation degrees.

Keywords: Perkins AD3.152UR engine, heat emission

INTRODUCTION

Ever steeper requirements faced by modern internal combustion engines are forcing manufacturers to use complex fuel cleaning systems as well as systems which improve the engine performance characteristics such as power, torque or a reduction in fuel consumption [8, 6, 7]. The shape of an indicator diagram has a direct impact on the values of those parameters. The diagram in question depicts the end result of thermodynamic, thermochemical and hydro-aerodynamic processes as well as heat exchange which occur in a cylinder of a piston internal combustion engine [1, 4, 5]. It is the primary quantitative and qualitative source of information on these processes and indicated engine performance parameters. Furthermore, it can be used to determine the heat emission characteristics during the combustion process, the equilibrium content of the working medium which changes in accordance with the crankshaft rotation angle function, "pressure increase in cylinders" of a working engine expressed as $dp/d\alpha$, etc.

The shape of the curve mostly depends on the progress and quality of fuel dispersion during the injection process as well as the quantity and aerodynamic properties of air in the engine cylinder, etc. These parameters are key when it comes to the quality of the created and combusted combustible mixture. A well organised combustion process impacts the conversion quality of chemical energy stored in the fuel into mechanical energy, fuel consumption, concentrations of harmful substances in the emissions and engine noise. The primary engine fuel combustion process characteristics are characteristics pertaining to the relative heat emission quantity. The form of the aforementioned characteristics is traced out on the basis of an analysis of actual indicator diagrams, which depends both on the accuracy of the diagram itself as well as the analysis method.

The relative heat quantity emission during the combustion process characteristic is determined on the basis of an indicator diagram analysis using the 1st law of thermodynamics [1]. Determination of the heat quantity emission during the combustion process characteristics requires the following to be known: a precisely recorded and plotted pressure change in a cylinder curve, instant cylinder volume, knowledge of the quantity, composition and properties of the working medium and a reliable model for the heat exchange between the working medium and cylinder walls. Preparing an experimentally taken indicator diagram for analysis has to entail a smoothing out of averaged pressure cycles in a cylinder and take into account precise and reliable determination of the piston position at TDC.

2. TEST SUBJECT AND TEST STAND

Experimental tests were carried out on an engine test stand which comprised an AD3.152 UR engine (test subject), brake, control and measurement cabinet, used to control the stand and obtain readings of the measured engine operation and brake parameters. The stand was equipped with a system for measurement of rapidly changing values such as: cylinder pressure, fuel pressure in the injection hose and injector needle travel. Figure 1 shows a diagram of the test stand.

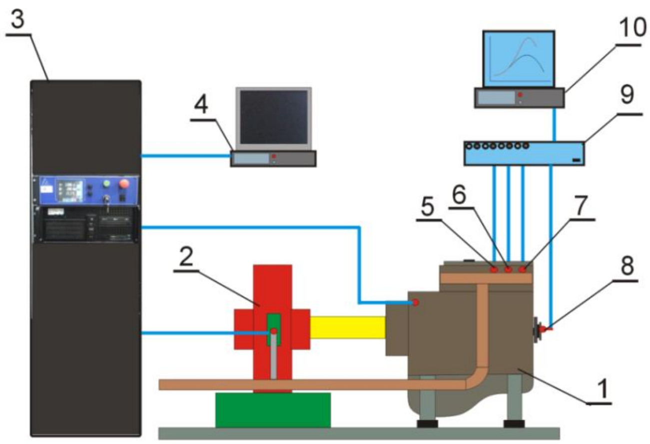

Fig. 1. Test stand, where: 1 - Perkins AD3.152UR engine: 2 - eddy current brake, 3 - measurement cabinet with test stand control system, 4 - computer used to control test facility parameters and to archive test results, 5 - engine cylinder pressure sensor, 6 - injector needle travel sensor, 7 - pressure sensor in the injection hose, 8 - engine crankshaft rotation angle encoder, 9 - module for measuring rapidly changing values, 10 - computer used to archive rapidly changing value readings

Figure 2 depicts a flow chart of the engine indication system. The system for measuring rapidly changing values comprise four measurement paths: combustion chamber pressure measurement path, injection hose pressure measurement path, injection needle travel measurement path, crankshaft rotation angle decoder path. The combustion chamber pressure measurement path comprised a liquid cooled piezo-quartz sensor, connecting leads and load amplifier. Injection hose pressure measurement path elements include a piezo-quartz sensor, connecting leads and load amplifier. The injector needle travel measurement path comprises: a linear variable differential transformer, connecting leads and an amplifier with a carrier wave. The values measured using the aforementioned sensors were recorded as a crankshaft rotation angle function. This task of the metering system was performed by the crankshaft rotation angle measurement path. This path included a crankshaft rotation angle transmitter and an electronics module, which initiated given measurement commencement impulses and generated a series of impulses ensuring readings every, defined engine crankshaft rotation angle range. The load amplifiers enhanced and processed signals generated by the sensors into voltage signals. Voltage signals were processed by an analogue - digital converter to into a digital format saved to the computer's memory.

OBJECTIVE AND SCOPE OF THE TESTS

The objective of the tests was to determine the impact of the angle of injection on the combustion process, evaluated on the basis of primary heat emission parameter characteristics. To that end, actual indicator diagrams were recorded over time as well as values required to calculate the primary engine operation parameters. During the test the engine operated according to an external speed characteristic. The variable parameter in the form of fuel angle of injection was 13, 17 and 21 crankshaft rotation degrees respectively. Based on the actual indicator diagrams identified during the tests as well as the primary engine operation parameters, heat emission characteristics during the combustion process were determined and then analysed. During the tests the engine was fuelled by diesel. See table 2 for its primary physical and chemical properties.

Table 2. Perkins 1104D-44TA compression-ignition engine specification

Parameter	Unit	Value
Cylinder system	-	inline
Number of cylinders	-	4
Type of injection	-	direct
Fuel system	-	Delphi DP310 rotary fuel injection pump
Maximum power	kW	75
Rated speed	rpm	2200
Maximum torque	Nm	416.0
Maximum torque rotational speed	rpm	1400
Displacement	m^3	$4.4 \cdot 10^{-3}$
Compression	-	18.2
Air inlet system	-	turbocharged, aftercooled

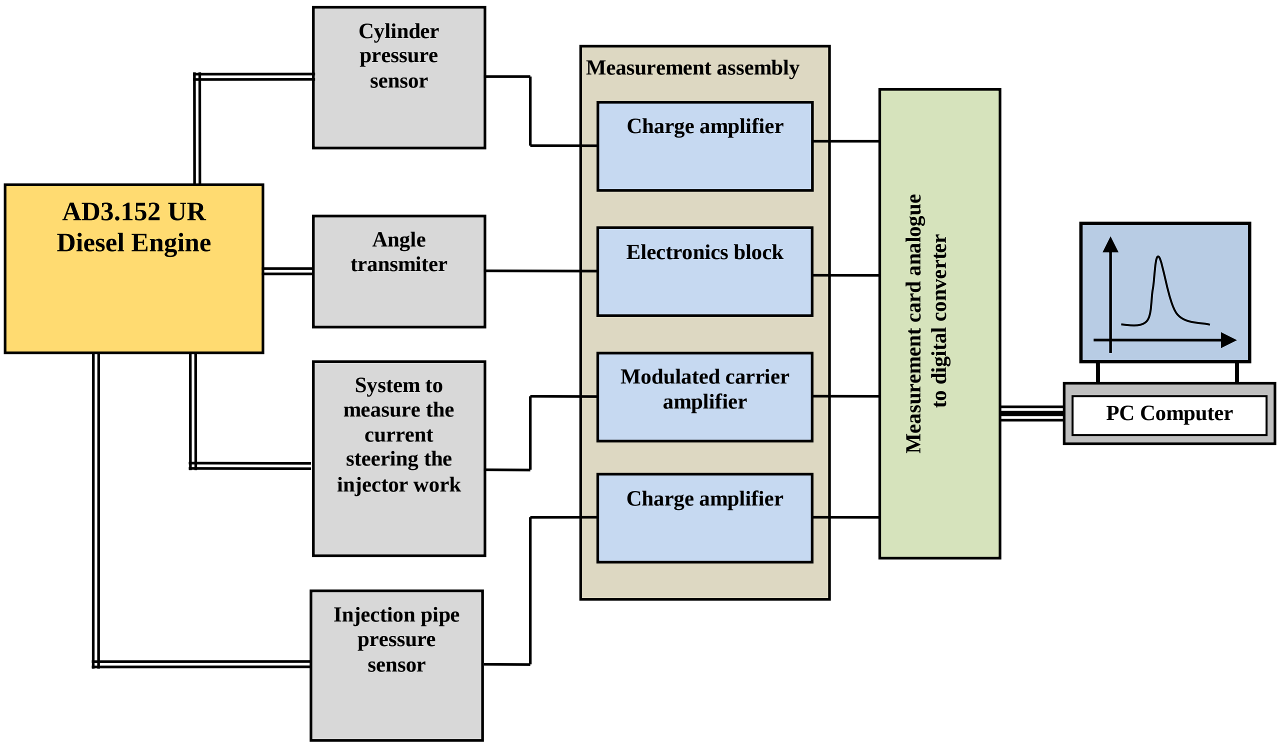

Fig. 2. Flow chart of the piston internal combustion compression - ignition engine rapidly changing parameters measurement system used for the experimental tests

Table 2. Primary physical and chemical properties of the fuel used to power the engine during testing

Parameter	Diesel
Cetane number	51.4
Net calorific value, [MJ/kg]	43.2
Density at 15°C, [g/cm^3],	0.8354
Kinematic viscosity, [mm^2/s] (~40°C)	2.64
Surface tension, [N/m] (20°C)	$3.64 \cdot 10^{-2}$
Ignition temperature, [°C]	63
Cloud point, [˚C]	-17
Cold filter plugging point, [°C]	-23
Average, elementary fuel composition, [%] - C - H - O	 87.2 12.7 0
S sulphur content, [mg/kg]	9
Water content, [mg/kg]	43.8
Solid contaminants content, [mg/kg]	5
Coking residue in a 10% distillation residue, [%(m/m)]	0.01
Copper strip corrosion test, [class]	1

HEAT EMISSION CHARACTERISTICS DETERMINATION ALGORITHM

Characteristics for the emitted heat during the combustion process were drawn up based on actual indicator diagrams. These characteristics were determined using the amount of fuel combusted during a cycle and the quantity of the working medium required to perform a cycle and excess air coefficient. Characteristics for the relative amount of emitted heat during the combustion process were drawn up on the basis of INDY-2 software developed at the Kielce University of Technology's Heat Engine Department [1]. Using the software in question, heat emission characteristics calculations are performed under the assumption that the combustion process terminated by the time the exhaust valve opens and that the total value of the relative heat amount emitted during the combustion process is equal to one.

Once the consumed fuel dosage during a cycle and working medium for that have been determined together with the excess air coefficient, the characteristic for the relative amount of emitted heat is determined on the basis of the first law of thermodynamic equation in the following format:

$$g_c W_u dx - \delta Q_{sc} - \delta Q_{nied} - \delta Q_{dys} = dU + pdV, \quad (1)$$

where

$$\delta Q_{sc} + \delta Q_{nied} + \delta Q_{dys} = \delta Q_{str} \quad (2)$$

or in an integral format:

$$g_c \cdot Wu - Q_{\sum str} = \Delta U + \int_{V_{ps}}^{V_{ow}} pdV, \quad (3)$$

where $Q_{\sum str}$ is a total heat loss transferred to cylinder walls and losses caused by thermolysis, imperfect and incomplete combustion, δQ_{sc} is a heat loss transferred to cylinder walls, δQ_{nied} is a loss caused by imperfect and incomplete combustion, δQ_{dys} is a losses caused by thermolysis, dU is a internal energy change, pdV is a work, W_u is a fuel net calorific value, g_c is a fuel quantity combusted during one cycle. That quantity was calculated using the following formula:

$$g_c = \frac{G_h}{30 \cdot n \cdot c} \text{ ; kg/cycle,} \tag{4}$$

where G_h is a hourly fuel consumption, n is an engine crankshaft rotational speed, c is a number of cylinders.

With knowledge as to the elementary fuel composition, M_o theoretical quantity of air required to combust 1 kg of fuel was calculated, and then with knowledge of λ excess air coefficient, the amount of M_1 kmol working medium for a single engine cycle was calculated using the following formula:

$$M_1 = g_c \lambda M_o \text{ ;} \qquad \text{kmol/cycle} \tag{5}$$

Dividing equation (1) by $g_c W_u$ we obtain a formula which can be used to determine the indicated net heat emission amount characteristics for the combustion process:

$$dx - \delta x_{str} = dx_i \tag{6}$$

where

$$dx_i = \frac{dU + \mathrm{pdV}}{\mathrm{g_c} \cdot \mathrm{Wu}} \, . \tag{7}$$

The equation can be written in the following format:

$$x - x_{str} = x_i \tag{8}$$

where

$$x_i = \frac{U_i - U_{ps} + \int_{V_{\alpha_{ps}}}^{V_i} pdV}{g_c \cdot W_u} \, , \tag{9}$$

where x is a relative amount of heat emitted during the combustion process, x_{str} is a relative working medium heat loss during the heat combustion process, x_i - indicated heat emission characteristic, V_i is current value at i^{th} point in the graph, $V_{\alpha ps}$ is a cylinder volume at the point corresponding to the start of combustion.

The maximum x_{imax} value is also the ξ utilisation coefficient of heat emitted during the combustion process.

In (9), U_{ps} is the working medium internal energy at the start of the combustion process, and U_i is the instant working medium internal energy , calculated using:

$$U_i = M_i \bar{c}_{vi} T_i \, , \tag{10}$$

where T_i is a current temperature M_i is a current working medium kmol in the engine cylinder during the combustion process, calculated using:

$$M_i = \beta_x M_{ps}; \quad where: \quad \beta_x = 1 + \frac{\beta_o - 1}{1+\gamma} \cdot x \, . \tag{11}$$

In that equation, β_x is the instant value of mole change coefficient.

The current value of mole specific heat capacity of the working medium during the combustion process in equation (10) is determined assuming a linear relationship with temperature, that is using:

$$\bar{c}_{vi} = a_i + b_i \cdot T_i \, , \tag{12}$$

The current values of specific heat capacities of the working medium during the combustion process is calculated using:

$$a_i = a_{spr}(1-x) + x a_\gamma \text{ ; } b_i = b_{spr}(1-x) + x b_\gamma \tag{13}$$

where T_i is the current temperature value calculated using state-space representation equations. When calculating the mean temperature as well as the work performed by the working medium, pressure values determined using interpolation functions are used.

The values of specific heat capacities coefficients of the working medium during the compression phase is calculated using:

$$a_{spr} = \frac{a_\lambda + \gamma a_\gamma}{1+\gamma} \quad i \quad b_{spr} = \frac{b_\lambda + \gamma b_\gamma}{1+\gamma} \, , \tag{14}$$

where a_λ and b_λ is the specific heat capacity coefficient for air, γ is an exhaust residue coefficient, a_λ and b_λ are the mole specific heat capacities of exhaust gasses generated by the combustion process.

With knowledge of x_i, characteristic of the relative net heat quantity emitted during the combustion process, the heat emission rate during combustion is calculated:

$$\dot{x}_i = \frac{x_i - x_{i-1}}{\alpha_i - \alpha_{i-1}} \, . \tag{15}$$

Figure 3 depicts a textbook run of the relative heat quantity emission rate during the combustion process characteristic with the share of combustion which proceeds according to the kinetic combustion model and share of combustion which proceeds according to the diffusion model identified.

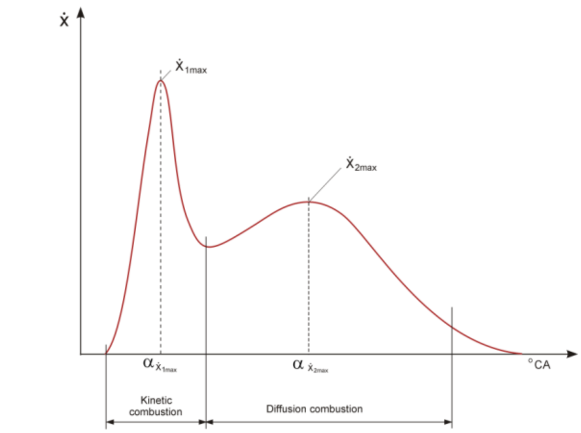

Fig. 3. Example relative heat emission rates during a combustion process with the x_{kin} kinetic combustion phase and x_{dys} diffusion phase identified together with the phases of their occurrence $\alpha\dot{x}_{1max}$ and $\alpha\dot{x}_{2max}$

Figure 4 depicts a graphical illustration of the presented methodology for determining the heat emission characteristic during a combustion process.

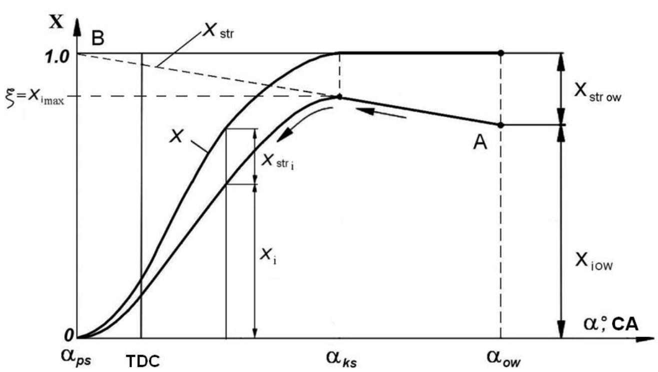

Fig. 4. A graphical illustration of the method for determining characteristic x, x_i and x_{str}: α_{ps} - start of the combustion process, α_{ks} – end of the combustion process, α_{ow} – engine exhaust valve begins to open

TEST RESULTS

The self-ignition delay period was determined by defining the start of the combustion process as the point where the curve of that indicated graph separates from the compression process curve (without the occurrence of the combustion process) drawn up for politropic exponent n_1, whereas the start of fuel injection was defined on the basis of h_i injector needle travel.

Figure 5 depicts the α_{os} injection angle for three angles of injection α_{ww} = 13, 17 and 21 crankshaft rotation degrees before the top dead centre TDC position of the piston and subject to engine operation according to an external speed characteristic. As can be seen on the diagram, a reduction of the angle of injection to 13 results in a decreased self-ignition delay, whereas increasing α_{ww} to 21 crankshaft rotation degrees results in a larger self-ignition delay relative to the nominal angle of injection of α_{ww} = 17 crankshaft rotation degrees.

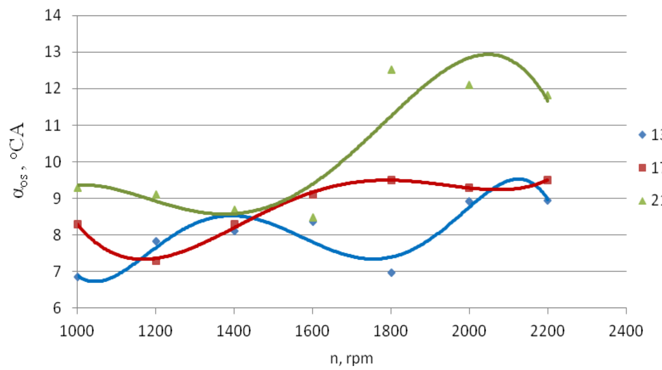

Fig. 5. Change to α_{os} angle of self-ignition delay under the engine operating according to an external speed characteristic for three fuel angles of injection α_{ww} = 13, 17 and 21 crankshaft rotation degrees.

Table 3 presents the primary combustion process parameters for the AD3.152UR engine operating according to a speed characteristic, for three angles of injection and powered by diesel. The table presents parameters such as N_e - engine brake horsepower, α_{os} - self-ignition delay, x_{kin} - kinetic model combustion proportion, x_{dyf} - diffusion model combustion proportion, $\dot{x}_{1max}$ - first flame speed, $\dot{x}_{2max}$ - second flame speed, $\alpha\dot{x}_{1max}$ - first flame speed engine crankshaft rotation angle, $\alpha\dot{x}_{2max}$ - second flame speed engine crankshaft rotation angle, x_{str} - relative heat losses

Figure 6 below depicts example graphs of heat emission characteristics for the of AD3.152UR engine fuelled by diesel under engine operation according to an external speed characteristic, for engine crankshaft rotational speeds n = 1400 and 2000 rpm and factory set angle of injectionα_{ww} = 17 crankshaft rotation degrees.

Figures 7 to 9 depict the primary combustion process parameters such as the proportion of kinetic model (x_{kin},) and diffusion model (x_{dyf}) combustion, value of first and second flame speed ($\dot{x}_{1max}$ and $\dot{x}_{2max}$) in an engine operating under an external speed characteristic for three angles of injection SUMMARY

One of the primary engine fuel combustion process characteristics is the characteristic pertaining to the relative heat emission quantity. The conducted analysis of measurement results and calculations demonstrated a clear impact of the fuel angle of injection on the primary characteristic heat emission characteristics quantities. Increasing the angle of injection resulted in a clear increase in the proportion of kinetic model combustion and a reduction to the diffusion model combustion. It also results in increased heat losses to combustion chamber walls. A change in the angle of injection has a slight impact on the maximum heat emission rates and the phases of their occurrence.

.

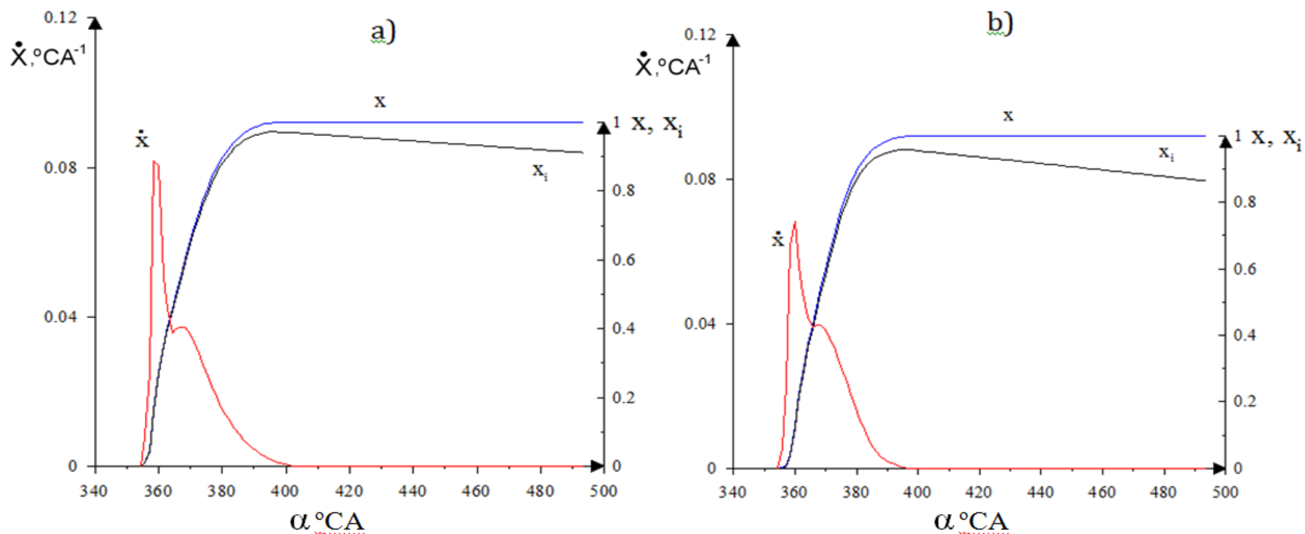

Fig. 6. Characteristics for relative heat emission during a combustion process x(α), x_i(α) and $\dot{x}$ (α) under the engine operating at the factory set angle of injection α_{ww} = 17 crankshaft rotation degrees and operating according to an external speed characteristic with a) n=1400 rpm and b) n=2000 rpm and fuelled by diesel.

Table 3. Combustion process parameters in an AD3.152 UR engine operating according to an external speed characteristic for three fuel angles of injection α_{ww} = 13, 17 and 21 crankshaft rotation degrees fuelled by diesel.

Lp.	n	α_{ww}	N_e	α_{os}	x_{kin}	x_{dyf}	$\dot{x}_{1max}$	$\dot{x}_{2max}$	$\alpha\,\dot{x}_{1max}$	$\alpha\,\dot{x}_{2max}$	x_{str}
	rpm	°CA	kW	°CA	-	-	$(°CA)^{-1}$	$(°CA)^{-1}$	°CA	°CA	-
1	1000	13	16,02	6,86	0,299	0,701	0,083	0,039	354,37	363,89	0,133
		17	16,50	8,3	0,496	0,504	0,127	0,031	355,78	367,03	0,116
		21	15,62	9,29	0,424	0,576	0,122	0,028	351,56	365,62	0,214
2	1200	13	19,72	7,82	0,311	0,689	0,08	0,041	355,78	364,53	0,132
		17	19,93	7,3	0,501	0,499	0,111	0,034	357,20	365,55	0,117
		21	19,12	9,11	0,453	0,547	0,105	0,028	354,37	365,62	0,197
3	1400	13	23,15	8,11	0,325	0,675	0,077	0,041	357,18	365,62	0,134
		17	23,40	8,3	0,487	0,513	0,099	0,036	357,17	367,03	0,138
		21	22,13	8,6	0,447	0,553	0,098	0,03	355,78	365,62	0,186
4	1600	13	25,96	8,36	0,395	0,605	0,070	0,042	358,59	367,22	0,153
		17	26,58	9,1	0,443	0,557	0,096	0,041	358,38	366,00	0,103
		21	25,16	8,48	0,476	0,524	0,095	0,034	355,78	367,22	0,222
5	1800	13	28,83	6,98	0,385	0,615	0,060	0,045	360,00	368,73	0,148
		17	29,53	9,5	0,496	0,504	0,083	0,039	360,00	371,25	0,117
		21	27,35	12,51	0,483	0,517	0,08	0,037	357,18	367,42	0,228
6	2000	13	30,37	8,93	0,256	0,744	0,053	0,047	361,40	368,43	0,141
		17	32,39	9,3	0,431	0,569	0,068	0,04	360,00	367,03	0,135
		21	29,55	12,11	0,437	0,563	0,067	0,039	358,59	365,62	0,218
7	2200	13	28,83	8,95	0,236	0,764	0,048	0,045	362,81	371,25	0,131
		17	26,78	9,5	0,299	0,701	0,052	0,044	360,00	369,84	0,195
		21	26,47	11,83	0,267	0,733	0,054	0,042	360,00	368,43	0,217

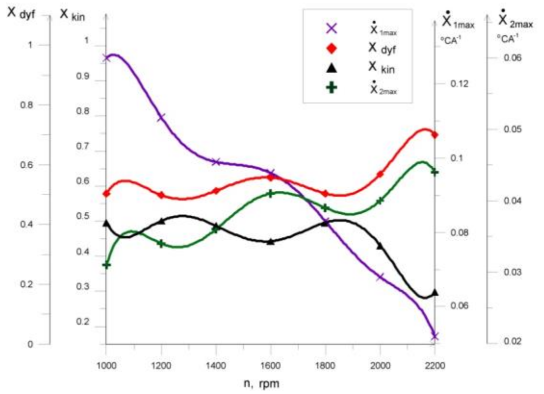

Fig. 7. Combustion process parameters for engine operation according to an external speed characteristic and angle of injection α_{ww} = 13 crankshaft rotation degrees, where x_{kin} is a proportion of kinetic model combustion, x_{dyf} is a proportion of diffusion model combustion, $\dot{x}_{1max}$ and $\dot{x}_{2max}$ is a first and second maximum heat emission rate

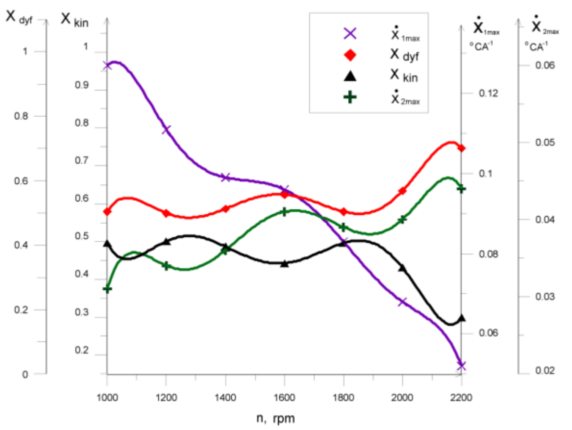

Fig. 8. Combustion process parameters for engine operation according to an external speed characteristic and angle of injection α_{ww} = 17 crankshaft rotation degrees, where x_{kin} is a proportion of kinetic model combustion, x_{dyf} is a proportion of diffusion model combustion, $\dot{x}_{1max}$ and $\dot{x}_{2max}$ are the first and second maximum heat emission rate

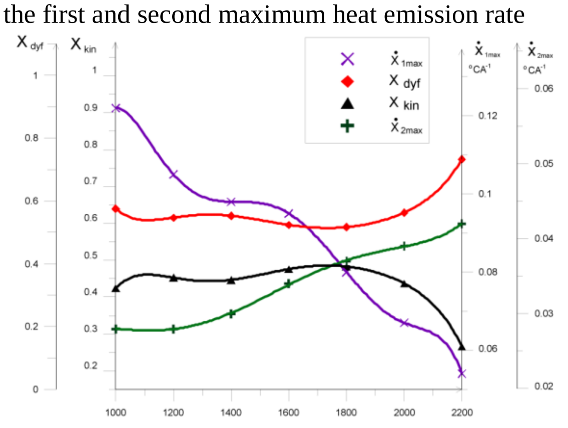

Fig. 9. Combustion process parameters for engine operation according to an external speed characteristic and angle of injection α_{ww} = 21 crankshaft rotation degrees, where: x_{kin} is a proportion of kinetic model combustion, x_{dyf} is a proportion of diffusion model combustion, $\dot{x}_{1max}$ and $\dot{x}_{2max}$ are the first and second maximum heat emission rate

REFERENCES

1. **Ambrozik A. 2010.** Analiza cykli pracy czterosuwowych silników spalinowych. Wydawnictwo Politechniki Świętokrzyskiej, Kielce.
2. **Ambrozik A., Ambrozik T., Łagowski P., 2008.** Aproksymacja rzeczywistego wykresu indykatorowego funkcjami sklejanymi. Zeszyty Naukowe Instytutu Pojazdów, Nr 2(69).
3. Łagowski P., 2010. Metodyka wyznaczania i ocena wielkości diagnostycznych wykresu indykatorowego silnika spalinowego o zapłonie samoczynnym. Praca doktorska, Politechnika Świętokrzyska, Kielce.
4. Ambrozik A., Kurczyński D., Łagowski P., 2005. Heat release characteristics in AD3.152 engine fuelled with hydrocarbon and biogenous fuels. First International Congress on Combustion Engines, PTNSS KONGRES – 2005, The Development of Combustion Engines, Bielsko-Biała/Szczyrk.
5. **Ambrozik A., Kruczyński S., Orliński P. 2007.** Ocena początku wtrysku paliwa na proces wydzielania się ciepła w silniku o zapłonie samoczynnym, Zeszyty Naukowe IP 3(66)/2007, Wyd. Politechniki Warszawskiej, Warszawa 2007, s. 99-106, ISSN 1642-347X
6. **Hyungmin Kim, Jeaduk Ryu, Kihyung Lee., 2007**. A Study on the Characteristics of Spray and combustion in a HCCI engine according to various Injection Angles and Timings. Journal of Mechanical Science and Technology, Vol. 21, No. 1, pp. 133 – 140.
7. **Lotko W., Longwic R., Górski K. 2002.** Ocena wpływu kąta dynamicznego początku tłoczenia paliwa na opóźnienie samozapłonu w silniku zasilanym olejami reformułowanymi, Międzynarodowa Konferencja Naukowa Journal of KONES 2002 (vol. 9), Warszawa – Gdańsk.
8. **Mysłowski J., Mysłowski J. 2008.** Próba poprawy wskaźników ekonomicznych silnika turbodoładowanego. Journal of KONES Internal Combustion Engines, Vol. 15, No. 3. 2008
9. Perkins Engines Company Limited: Technical Data 1100 Series. Industrial Open Power Until. 1104D-44TA 75,0 (Nett) @ 2200 rev/min Balanced. Perkins, England, 2008.
10. PN-EN 590:2013-12 Paliwa do pojazdów samochodowych. Oleje napędowe. Wymagania i metody badań.
11. User manual AVL DiCom 4000 PL.
12. **Serrano L., Lopes M., Pires N., Ribeiro I., Cascao P., Tarelho L., Monteiro A., Nielsen O., Gameiro da Silva M., Borrego C. 2015.** Evaluation on effects of using low biodiesel blends in a EURO 5 passenger vehicle equipped with a common-rail diesel engine. Applied Energy 146/2015, s. 230–238.
13. **Tys J. i in. 2003:** Technological and economic determinants of rapeseed biofuels production. Instytut

Agrofizyki im. Bohdana Dobrzańskiego PAN w Lublinie. (in Poland).

14. **Wcisło. G. 2010:** Utilization of used oils and fat for manufacturing FAME biofuels. Teka Komisji Motoryzacji i Energetyki Rolnictwa, 2010, Vol. X, s. 509-516. 2010. (in Poland)
15. **Wcisło. G. 2010:** Processing of biomass for energy purposes. Collective work edited by Frączek J. University of Agriculture. H. Kołłątaja, Kracow. 85-146.
16. User manual AVL DiCom 4000 PL.
17. Law of 25 August 2006 on the fuel quality monitoring and control system (Dz.U. 2006 Nr 169, poz. 1200). (in Poland)
18. **Wcisło G. 2017.** Determining the effect of the addition of bio-components AME on the rheological properties of biofuels. Econtechmod: an international quarterly journal. Volume 6, № 1. 105-110.
19. **Wcisło G., Labak N. 2017.** Determination of the impact of the type of animal fat used for production of biofuels on the fractional composition of AME. Econtechmod: an international quarterly journal. Volume 6, № 1. 111-114.
20. **Kurczyński D., Łagowski P., Wcisło G., Pracuch B., Tomyuk V.** Ecological indicators for the Perkins 1104D-44TA engine fuelled by sunflower oil methyl esters operating according to load characteristics. Econtechmod: an international quarterly journal. Volume 6, № 4. 71-80.
21. **Kurczyński D., Łagowski P., Wcisło G., Pracuch B., Leśniak A. 2017.** External speed characteristic for the Perkins 1104D-44TA engine fuelled by sunflower oil methyl esters. Econtechmod: an international quarterly journal. Volume 6, № 4. 111-120.